SIN-CHN
SCIENTIFIC PRESS PTE.LTD.

Molecular & Cellular Biomechanics 2024, 21(2), 352.
https://doi.org/10.62617/mcb.v21i2.352

Article

Lightweight aircraft design: Integrating biomechanics and algorithm optimization for drone construction using paper materials

Jiazheng Wang, Parvathy Rajendran*

School of Aerospace Engineering, Universiti Sains Malaysia, Engineering Campus, Nibong Tebal, Pulau Pinang 14300, Malaysia
*** Corresponding author:** Parvathy Rajendran, aeparvathy@usm.my

CITATION

Wang J, Rajendran P. Lightweight aircraft design: Integrating biomechanics and algorithm optimization for drone construction using paper materials. Molecular & Cellular Biomechanics. 2024; 21(2): 352. https://doi.org/10.62617/mcb.v21i2.352

ARTICLE INFO

Received: 11 September 2024
Accepted: 23 September 2024
Available online: 6 November 2024

Abstract: Lightweight aircraft design emphasizes materials like composites, alloys, and advanced polymers to reduce weight while ensuring structural integrity. Streamlined aerodynamics, efficient propulsion systems, and optimized component layout further enhance performance. The purpose of this research is to develop an innovative aircraft design model for drones, integrating algorithm optimization techniques and lightweight materials to enhance the performance and efficiency of drones with the utilization of open-source software. We apply this structure to the construction of drones with fixed-wing (FW) and vertical take-off and landing (VTOL) configurations. The aircraft's body is constructed using lightweight materials such as glass fiber fabric (Gff) and extruded polystyrene foam (XPS), employing a vacuum-assisted wet layup technique for fabrication. Multi-objective Co-evolving Ant Colony Optimization (MC-ACO) was used to improve the construction of drones with VTOL and FW capabilities. This strategy enabled it to be easier to achieve the trade-offs required for a generalist drone design, such as range, payload capabilities, and swarm operations, which were then evaluated against commercially available software to evaluate the effectiveness. Incorporating biomechanics into the design method permits higher consideration of user interaction with drones. The findings indicate that low-fidelity architecture is a suitable starting point for prototyping under limited time frames. The paper concludes with a discussion of the technical constraints of employing free software, as well as some practical concerns for flight testing drones with hybrid configurations.

Keywords: lightweight aircraft; biomechanics; constructing drones; Multi-objective Co-evolving Ant Colony Optimization (MC-ACO); lightweight materials

1. Introduction

The last decade has seen exponential growth in technological advancement and the diversity of applications of unmanned aerial vehicles (UAVs), otherwise commonly referred to as drones. Invented for military objectives, drones have outgrown their original functions to take form as basic assets in civilian activities ranging from agriculture, real estate, and environmental monitoring to delivery services [1]. The quickly expanding space of drone applications underscores the need for further development in drone design and functionality to enlarge [2], in particular, flight duration, payload capacity, and operation efficiency.

One of the major challenges of drone technology is to find the right compromise between weight and structural strength [3]. The second reason for such a design to be lightweight is that it directly affects the performance of the drone in terms of basic metrics such as battery life, flexibility, and the possibility of additional sensor loads or payloads. Traditionally, high strength-to-weight ratios were achieved through composites, alloys, and advanced polymers [4]. However,

these materials generally tend to be more expensive and complicate the processes of manufacturing and recycling. The introduction of new materials, such as XPS and Gff [5], which have only recently been developed and used, presents a weight reduction coupled with large cost savings. The characteristics of these new materials, XPS and Gff, are certainly bound to be lightweight and allow complex geometrical configurations of the design to achieve aerodynamic efficiency in drones [6].

The ability to utilize the latest optimization algorithms, to develop and optimize design parameters at a level not achievable by traditional trial-and-error techniques [7]. Through an optimization algorithm, these functions deal with many design objectives that very commonly have conflicting characteristics [8], such as maximum range versus payload, as well as minimum weight and cost. The use of such algorithms within a design process allows efficient exploration of large design spaces, which paves the way for innovative approaches that can be tailored according to specific application needs [9]. Integrating biomechanics into design opens up similarly possibilities, in particular for applications requiring ergonomic concerns, or specialized uses. The development in drone design at present is also demanding tools that are not only sophisticated but also accessible. Technology is made more accessible to everybody by using open-source software to develop and evaluate drone performance [10]; researchers, hobbyists, and small enterprises can engage in and benefit from the development of drone technology without expensive commercial software.

The achievement of this study is a contribution to the intensive investigation of the drone design field by using both advanced lightweight materials and multi-objective optimization algorithms. The purpose of this paper is to boost the efficacy of drones so that they can take care of the rising number of various practical uses by supplying sustainable and powerful drones. This writing focused on the process and the results of using a unique design adapted in the MC-ACO way and fabricated with custom-made modern and cost-effective materials at the front line of the lightweight drone design.

Key-contribution

- Utilized advanced lightweight but strong materials such as XPS and Gff, drastically reducing the drone's weight and manufacturing costs.
- Deployed MC-ACO to achieve superior trade-off solutions in performance-critical design objectives such as range, payload, and efficiency.
- Used only open-source applications for design and evaluation, allowing the technology to be easily and quickly adopted and scaled, free of charge from the high costs of proprietary tools.

Five primary components comprise the paper: Section 1 offers an introduction, while Section 2 presents relevant research from our work. Section 3 provides specifics on the configuration selection, initial design phases, and optimization strategy utilizing MC-ACO. Based on simulations and empirical data, Section 4 presents the results of the optimization, observations from flight testing, and system dynamics. Section 5 concludes the paper.

2. Literature review

Study [11] used material composite strengthened with glass and carbon fiber to construct a drone subcarrier. Using optimization methods for slime mold, gray wolf, and genetics, the ideal stacked angle was found. The carrier's minimum displacement was more than 60 MPa, as was its stress value. According to the research, the slime mold method was the most effective method for determining the optimal values for artificial intelligence methods that estimate the stacked angle of material composites. The utilization of thin-layer materials in structures that bear loads was on the rise in the aerospace field, as noted by the author [12]. However, cautious planning was necessary to minimize load capacity and reduce stability. Utilized a model that generated techniques, a program was created to suggest and assess those designs; Finite Element Technique research was then employed to confirm and enhance them. The research advanced the design of automated lightweight and extremely flexible airplane structures. Researchers from [13] highlighted the way Unmanned Aerial Vehicles (UAVs) have advanced transcend military usage to encompass search and rescue and the Coast Guard. With an emphasis on long-term UAVs for life-saving applications, they evaluated the designs of rotors created by 3D printing. The authors examined alternative designs for rotor structure, loading, and effective rotor part arrangement. Multiple materials were employed for optimal strength and stress testing got the best results. Article from [14] concentrated on employed commercial programs and technical methods to improve an autonomous aerial vehicle's pylon installation. The complicated design was generated as Ti-6Al-4V utilized the Electron Laser Heating technique. The outcome showed a technical plan for minimized weight campaigns and produced a lightweight, galvanic fitting design that was suitable with carbon composite basic components. Article [15] used 3D printing and topology optimization to develop and manufacture lightweight micro-UAVs. Finite element modeling was used to describe and verify Nylon 12's characteristics as a material. A Z-split arrangement was designed through optimization of topology, confirmed by stress testing and 3D fabrication. The study made an argument for the secure and reliable application of such advances in the design and development of micro-UAVs. Study [16] aimed to develop a compact quadcopter framework for UAVs to enhance flight capabilities. The study found a compromise between reducing weight and structural strength by utilizing lightweight supplies, 3D printing, and sophisticated creative design approaches. Similar to the DJI F450 drone, the discovery resulted in weight savings of nearly 50%, higher P/W and T/W ratios, and shorter production times. Those findings have implications for careful farming and aerial robotics. Using generative design and additive manufactured technologies, the author of [17] investigated drone optimization. The use of additive manufacturing enabled complicated designs and allowed for weight reduction while preserving drone body strength. 3D printing and Finite Element Method (FEM) analysis might detect overdrawn regions, allowing for material removal or design adjustments. The objective was to reduce drone mass, hence lowering energy consumption and lift power. To achieve a higher rotor distance-to-weight ratio and take-off weight, the study contrasted five commercial drones with a 3D-printed prototype.

Researchers in [18] talked about how technology for solar panels and additive printing can be used to design and build a fixed-wing aircraft. Enhanced the skills of the aviation sector, increasing the number of autonomous tasks, and produced durable aircraft with superior mechanical attributes were the objectives. The study also suggested minimum surfaces for reinforcing UAV wings. Also displayed was the SolarÍO proposal for a solar-powered airplane. Article [19] compared five common drone development materials such as aluminum alloy, carbon fiber reinforced plastics, polystyrene, balsa wood, and Kevlar. It was determined which material would work best for developing the wing structure using the suggested approach. To evaluate deformation and vibration resistance, structural and vibration analysis was done. Comparing popular materials and taking key characteristics into account, the study wanted to help researchers choose the most effective material. Author of [20] published findings from Carleton University's Blended Wing Body (BWB) UAV team. The group used the Multiscale Design Optimization (MSDO) method to create and improve a clean sheet UAV with BWB layout while taking manufactured limitations into account and utilized lattice components. Critical loads were computed, stress was analyzed and the design was optimized. The researchers discovered weight reductions of 36.44% and 59.65% for MSDO and topology optimization, respectively, indicated that MSDO was a viable substitute for applications that need precise weight measurements. Research of [21] suggested a micro-lattice reinforcement approach employed dual-phase reinforcing in crystallizing, combined stretching-dominated octet-trusses into the bending-dominated body-centered cubic lattice matrix. Enhanced stiffness, absorption of energy, and improved specific strengths of compression were the results of the method. A micro aerial vehicle was successfully equipped with a large-scale octet-truss body-centered cubic (OCT-BCC) lattice met material, which led to a lighter airframe and longer flying times.

Researchers at [22] utilized transdisciplinary optimization methods to create a morphing variable span tapered wing (MVSTW) utilizing composite materials. To evaluate the viability of morphing wing optimization, topological optimization, structural scaling, and material selection were all examined in the study. To achieve structural rigidity demands, the wing components were designed to be lightweight while remaining stiff. At only 5.5 kg, the MVSTW was a lot lighter and it was able to fly missions without experiencing any mechanical failures. A hybrid UAV design with a good thrust-to-weight ratio for tiny multi-rotor UAVs was received in the research of [23]. An innovative convergent-divergent (C-D)-based duct that was recently redesigned was used in the propeller's layout to boost efficacy. The structural and mechanical aspects of the layout were greatly reduced. The best-performing material for the UAV's layout was alloyed titanium which was picked using modeling software and Computer-Aided Three-dimensional Interactive Application (CATIA). Applications including monitoring in restricted spaces, detection, inspection, and surveillance were appropriate for the hybrid UAV. Study [24] developed a rotary-wing unmanned aerial system (RUAS) to detect contaminants and reduce their level in the atmosphere. To assure both the environmental and technical benefits of the RUAS, sophisticated methods for computational and simulated composite development of materials were utilized, such

as fluid-structure interaction, integrated engineering, and computational moldings assessments. The objective of the [25] research was to use additive manufacturing design, topology optimization, and part consolidation to re-engineer the frame into a monocoque structure, therefore reducing both frame weight and structural integrity in commercial UAV designs. When contrasted with commercial UAV designs, the re-engineered Quadcopter structure produced using Fused Filament Fabrication demonstrated greater operational supremacy and durability.

3. Methodology

3.1. Paper materials

Paper material in the context of lightweight aircraft design, specifically for drones, confer with using diverse forms of paper and paper-based totally composites as strutural additives. These substances can encompass conventional papers, bolstered paper products, or specially treated paper designed to decorate power and sturdiness while keeping a lightweight profile. While paper substances can be lightweight, they will no longer continually healthy the power and durability of other materials like carbon fiber or aluminum. If the paper is sourced domestically and produced with environmentally friendly processes, it may contribute to a reduced carbon footprint compared to materials that require full size transportation or excessive energy manufacturing. The paper materials used in lightweight aircraft design are as follows.

- Cardstock
- Kraft paper
- Treated paper
- Honeycomb paper bond
- Laser cut paper
- Paper composites
- Pulp-based composites
- Origami structures

Lightweight aircraft material

These are commonly used for recreational flying, training, and specialized applications consisting of agricultural obligation and emergency services. The creation of lightweight aircraft frequently entails superior materials follow as:

- Aluminum alloy
- Titanium alloy
- Composite materials
- Magnesium alloy
- Foam and laminates

Lightweight aircraft are increasingly incorporating electric propulsion and sustainable substances, paving the manner for environmental friendly aviation solutions.

3.2. Designing concepts

Setting high-level design requirements and project dates is the first phase in the system engineering process. The lightweight aircraft's flying range is optimized to 120 km by keeping its vertical takeoff and landing speed at 30 m per second. Target identification, vertical takeoff, cruised flight, cargo delivery, and surveillance will all be part of the aircraft's standard mission profile. Biomechanics can play a role in optimizing the interconnection between drones and operators. The supplementary material includes a video describing the theory of activities for the whole mission profile, considering the potential benefits of multiple comparable UAVs working together as a cooperative colony.

Choosing a configuration:A Pugh matrix analysis is used to determine the trade-offs for various configuration characteristics in a tri-copter design. The supplemental material includes weighted scores for each configuration, which are then compared and evaluated. Design experience and safety considerations are crucial in the selection process. The tri-copter has two forward tilting motors and a composite flying rotor arrangement. After takeoff, the primary for cruising flight, the motors tilt forward and back for landing. Waving motion can be controlled by directing motors along the pitch axis. The equation could be used to alter the total drag component of the UAV.

$$\left(D_{Cp}\right)_{total} = \left(D_{Cp}\right)_{x} + \left(D_{Cp}\right)_{gs}\frac{T_{gs}}{T} + \left(D_{Cp}\right)_{us}\frac{T_{gs}}{T} + \cdots \ldots + \left(D_{Cp}\right)_{uspk}\frac{T_{uspk}}{T} \qquad (1)$$

The equation (D_{Cp}) represents the overall rotor drag is zero-lift, $\left(D_{Cp}\right)_{gs}$ and $\left(D_{Cp}\right)_{us}$ represent both the vertical and horizontal tail zero-lift drags and $\left(D_{Cp}\right)_{uspk}$ compensates for the drag in other parts. Here T depicts the wetted areas of different parts, such as VTOL motors, tilt rotor systems, and the wetted flight area's ratios for aluminum struts. A blended flying rotor is ideal for long-duration missions due to its lower $\left(D_{Cp}\right)_{gs}$ component, improved winglet function to minimize vortex-induced drag, and general lower $\left(D_{Cp}\right)_{us}$ portion (Supplementary Material).

In terms of weight and reduced (S/W), a tri-plane that has 2 forward tilt motors is a very good option. In budget-conscious settings, the benefits of having more rotors are offset by their weight and expense, even though these lightweight aircraft offer improved airworthiness and stability. Thus, because a tri-copter arrangement requires less power, dead weight, and money, it was selected. Be aware that while these trade-offs are plausible conceptually, they do not give all the details and that predictions were verified or refuted by real flight testing on a working prototype frame.

Estimating weight:To begin estimating, historical data is analyzed, characteristics are collected and a hypothesis is developed using procedures similar to those in. To fit the data (supplementary material), a linear regression curve was developed based on the payload, which was determined within restrictions. To provide an acceptable forecast, the quadratic equation created by this trend line is solved analytically. It's noteworthy to see that the value of a is higher than fixed-wing values, which are usually attained around ≈ 0.9. This is consistent with

expectations and can be attributable to the increased weight of VTOL systems, which reduces aerodynamic efficiency.

$$\frac{X_f}{X_p = b \times X_p + a} \tag{2}$$

$$X_p = X_f + X_o \tag{3}$$

$$b = -0.00468; a = 0.887 \tag{4}$$

Based on the earlier analysis of regression, a projected total mass (X_p) of 7.79 kg is needed to transport 1 kilogram of payload (X_o). The empty weight (X_f) is 6.79 kg. The calculation includes a safety margin of 180 g to account for weight accretion, potential dead-weights, and experience after repairs due to collisions.

$$X_o = 1kg \tag{5}$$

$$Xp = 6.84 + 0.16 \approx 9kg \tag{6}$$

3.3. Preliminary design

A great deal of optimization mathematics is used in the initial design phase. Reducing power and increasing cruise efficiency are the two main goals of the method of optimization, which aims to create the widest range possible in terms of geometry and propulsion. We have separated the design and optimization procedure into several stages for this instance.

3.3.1. Initial dimensions

Wing loading and power loading, which are the two main driving forces behind any design, are roughly estimated in the first step. To accommodate for disk loading, appropriate hover, climb and transition phases for tri-copter sizes are incorporated. Linear programming is used to construct a crude but mathematically sound approximation at this step. Therefore, we just provide brief overviews of the equations below. The plane's stalling point wing loading is found in Equation (7). Usually, the wing area's bottom bound is determined by this restriction. For high stall speeds and high cruise ceilings, Equation (8) could provide a lower bound. For optimizing endurance, rising at a specific rate (ROC), and shifting with $Vmax$ at sea level (SL) altitude, respectively, the ideal wing loadings are given by Equations (9)–(11). The values of $(K/C)_{max} = 11$, the aspect ratio AR = 8, the propeller efficiency ηo = 0.8, and the Ostwald's efficiency factor f = 0.8 are displayed below. Please keep in mind that these numbers, particularly for AR and $(K/C)_{max}$, are educated estimations that may need to be adjusted based on the actual outcome.

$$\left(\frac{X}{T}\right)_{stall} = 0.5\rho(U_{stall})^2 D_{K_{max}} \tag{7}$$

$$\left(\frac{X}{T}\right)_{maxrange} = r\sqrt{\pi(BQ)fD_{Co}} \tag{8}$$

$$\left(\frac{X}{T}\right)_{maxloiter} = r\sqrt{3\pi(BQ)fD_{Co}} \tag{9}$$

$$\left(\frac{X}{O}\right)_{ROC} = \frac{1}{\frac{ROC}{\eta_o}\sqrt{\frac{2}{\rho\sqrt{\frac{3D_{C_p}}{L}}}\left(\frac{X}{T}\right)\left(\frac{1.155}{\left(\frac{K}{C}\right)_{max}\eta_o}\right)}} \tag{10}$$

$$\left(\frac{X}{O_{TK}}\right)_{u_{max}} = \frac{\eta_o}{\frac{1}{2}\rho_p U_{max}^3 D_{C_p}\frac{1}{\left(\frac{X}{T}\right)} + \frac{2L}{\rho\sigma_{air}U_{max}}\left(\frac{X}{T}\right)} \tag{11}$$

The total area of the propellers used to create vertical thrust is calculated using the following formulas. This region is characterized by disk loading (DL), similar to wing loading. The propeller area during transition is calculated using Equation (14). The tilting angle (θ_{tilt}) affects this relation since it seeks to maintain a consistent speed as they go from hover to cruising mode. In this case, the angle is assumed to be fixed. However, another option is to investigate a changing angle at a steady pace, which is more in line with the way actual systems change.

$$\left(\frac{X}{O}\right)_{hover} = FOM\left(\frac{\sqrt{2\rho}}{CK}\right) \tag{12}$$

$$\left(\frac{X}{O}\right)_{climb} = \frac{1}{U_z - \frac{l_1 U_z}{2} + \frac{l_1}{2}\sqrt{U_z^2 + \frac{2(CK)}{\rho_p} + \cdots} \ldots + \frac{\rho_p U_{tip}^3}{(CK)}\left(\frac{\sigma D_c}{8}\right)} \tag{13}$$

$$\left(\frac{X}{O}\right)_{trans} = \frac{1}{c_1 + c_2 + c_3} \tag{14}$$

$$c_1 = \frac{l_1}{sin(\theta_{tilt})}\sqrt{\frac{-U_\infty^2}{2} + \sqrt{\left(\frac{-U_\infty^2}{2}\right)^2 + \cdots}} \ldots + \left(\frac{CK}{2\rho sin(\theta_{tilt})}\right)^2 \tag{15}$$

$$c_2 = \frac{\rho U_{tip}^3}{CK}\left(\frac{\sigma D_c}{8}(1 + 4.6\mu^2)\right) \tag{16}$$

$$c_2 = \left(\frac{1}{2}\rho_p - U_\infty^2 D_{C_p}\frac{1}{\left(\frac{X}{T}\right)} + \frac{2L}{\rho_p U_\infty}\left(\frac{X}{T}\right)\right) \tag{17}$$

Given the motors and their respective propeller diameters, a maximum and a minimum amount of disk loading are used as well to further restrict the study. Constricted by each of their ascent restrictions, the fixed-rotor and VTOL design points are separated. To ensure safety, the highest power points are specified for each arrangement.

$$T_{wing} = \frac{X_p}{(X/T)_{pos}} \tag{18}$$

$$O_{cruise} = \frac{X_p}{(X/T)_{EX}} \tag{19}$$

$$O_{USPK} = \frac{X_p}{(X/T)_{USPK}} \tag{20}$$

3.3.2. Geometry optimization

Preliminary estimates:To determine static stability characteristics, the lightweight aircraft's performance is initially calculated using XFOIL. Reynolds number and peak D_k / D_c values and stall characteristics at cruising altitude are used to guide reflexed airfoil design and initial improvement at different angles of attack. See the supplemental material for the techniques trade-off matrix. A Static lift evaluation is performed on the flying wing's operational Gross Takeoff Weight (GTOW) (**Figure 1A**), to achieve static stability. **Figure 1A** represents a simple top view of the initial flying wing layout. The wing is proven in a streamlined, triangular shape, similarly demonstrating its aerodynamic structure. This view highlights the geometric simplicity and symmetry in flying wing designs. It could be an early or conceptual layout that specializes in the general form without exact structural additives visible. The Center of Gravity (CoG) location was balanced to guarantee that the pitching moment was near 0 and iterations on the design variables were carried out to maximize the cruising velocity of the entire wing. The twist of the wing lowered its D_K, resulting in a larger wing area than expected. To guarantee consistency in performance estimations, an analysis is also conducted on a preliminary and conceptual approximation of the anticipated design (**Figure 1B**). It appears to be an extra specified, three-dimensional rendering of the flying wing. It consists of what view as if a cutaway or mesh model of the wing shape, showing internal information like cross-section or float lines. The extra complexity in this view likely represents a computational or analytical layout phase, that specializes in airflow analysis or structural optimization.

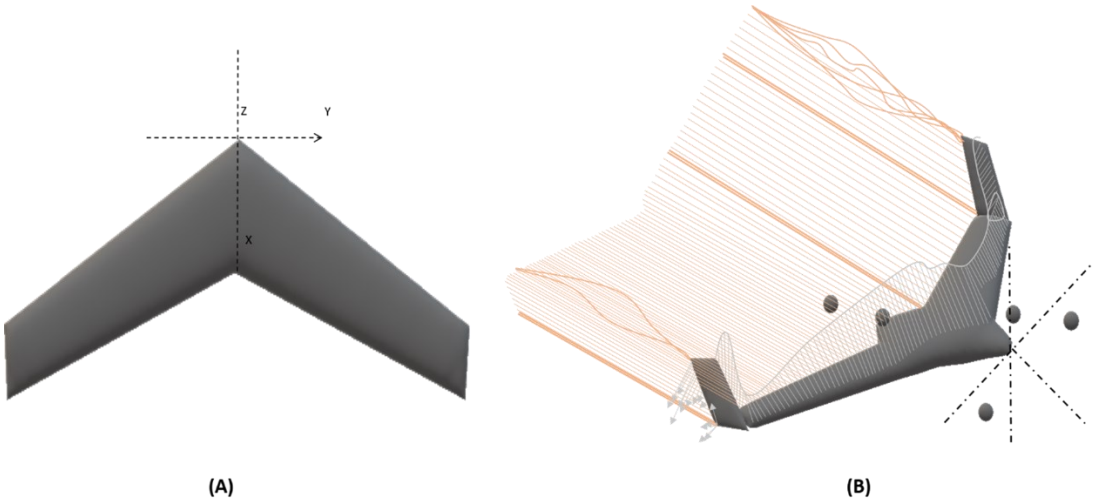

Figure 1. (A) initial designs; **(B)** aerial view of wing configurations.

Problem setup: Aiming to optimize the lightweight aircraft's geometry is the second stage. It is recognized that merging both phases might result in more optimal designs, even if this step is separated from propulsion selection to ease the construction of interfaces and debugging procedures. An MC-ACO technique is used since there are just a few variables, code development is simple, and pre-existing libraries are available. To more efficiently use high-fitness solutions, the MC-ACO's parameter settings are described in **Table 1**, which also includes generational modifications to pheromone decay and heuristic impact.

Table 1. MC-ACO parameter settings.

Parameter	Initial Values	Final Values	Method
Pheromone Amount	1.0	0.1	Exponential decay
Evaporation Rate	0.1	0.01	Exponential decay
Alpha (pheromone influence)	1	3	Linear increase
Beta (heuristic influence)	2	5	Linear increase
Number of Ants	20	50	Dynamic
Generations (N)	-	80	Constant

Every single objective's weighted total serves as the optimization's function of objectives (Equation (21)). To simplify, all weights (x) are regarded as equal but with opposing signs that indicate whether objectives need to be reduced or maximized. Four variables are used for setting up the problem: the leading edge sweep (Λ_{KF}), dimension ratio (AR), taper-ratio (λ), and root-tip twist (Θ_{rel}).

The following three elements are included in the combined objective function; Drag: A margin is added to the lift coefficient of the airfoil during cruising circumstances (Equation (24) to account for variations between a 3D rotor and a 2D cross-section. The study is carried out at this constant lift coefficient.Lift Distribution:The twist, taper ratio, and sweep all affect the real lift distribution (D_K^b). The load distribution's goal curve (D_K^b) is matched using a cost function using least squares. There is another Python script that is used to carry out this computation. Stability: While optimizing for stability often necessitates trade-offs with performance, the short-period damping ratios (τ_{TO}), Phugoid (τ_{OG}), and Dutch roll (τ_{CQ}) modes are included inside the objective. For stability in fixed situations, however, 2 constraints on the allowable static margin (Equation (25)) at 0 moments at the layout coefficient of lift (Equation (26)) are deemed sufficient. Coefficients of stability are derived from JSBSim's output, specifically tailored for flight dynamics modeling. The output from JSBSim simulations is converted into a data frame for more examination.

The values in constraint Equations (29)–(32) are determined by perceptible trends detected in the supplemental material.

$$Min_w \sum_{j=1}^{\#I} x_j I_j \tag{21}$$

$$I = \left\{ D_{C,} \frac{1}{m} \sum_{z=0}^{a/2} \left(D_K^s(z) - D_K^b(z) \right)^2 \tau_{TO}, \tau_{CQ}, \tau_{OG} \right\} \tag{22}$$

$$w = [BQ, \Theta_{rel}, \lambda, \Lambda_{KF}] \tag{23}$$

$$D_K = 0.9 D_j^d \tag{24}$$

$$T.N. = 4\% \tag{25}$$

$$T_N \approx 0 \tag{26}$$

$$D_K^s(\mathrm{z}) = Targetlift \tag{27}$$

$$D_K^b(\mathrm{z}) = Acutallift \tag{28}$$

$$5 \leq BQ \leq 10 \tag{29}$$

$$-1 \leq \Theta_{rel} \leq -5 \tag{30}$$

$$0.4 \leq \lambda \leq 0.9 \tag{31}$$

$$20 \leq \Lambda_{KF} \leq 30 \tag{32}$$

3.4. Propulsion system design and optimization

A flight's propulsion system is designed to maximize range and/or durability while enabling the flying machine to operate at peak performance.

Forward motors: Equations (36)–(40) was used to determine the ideal motor combination, propeller size, and pitch to produce the necessary performance when cruising at 25 m/s. During the cruising phase of flight, forward motors are necessary. The pitch speed of the engine, which was using the thrust necessary to maximize endurance and overcome drag while cruising, was matched to this area involved. **Figure 2** depicts the ideal thrust curve, which illustrates this strategy. A cruise drag D_{dc} was produced by the fixed-wing's original design, which the front cruise motors would need to overcome. Equation (35) uses a scaling factor Φ_c to compare cruising to the motor's likely Rotation per Minute (RPM) at S_{cruise} and S_{max}. Selecting the front motor parameters is provided in **Table 2**.

$$\Omega_{cruise} = \frac{60 v_{pitch}}{0.0254 w_{pitch}} \tag{33}$$

$$LU = \left[\frac{\Omega_{cruise}}{U} \Phi_d \right] \tag{34}$$

$$\Phi_d = \sqrt{\frac{S_{max}}{S_{cruise}}} \tag{35}$$

$$\upsilon_{pitch} = 25m/s \tag{36}$$

$$S_{cruise} = \frac{1}{2}\rho v^2 T D_c^d \tag{37}$$

$$U = 22.2u(6TBattery) \tag{38}$$

$$10.16cm \leq w_{pitch} \leq 20.32cm \tag{39}$$

$$0.6 \leq \left(\frac{S}{X}\right)_{max} \leq 0.8 \tag{40}$$

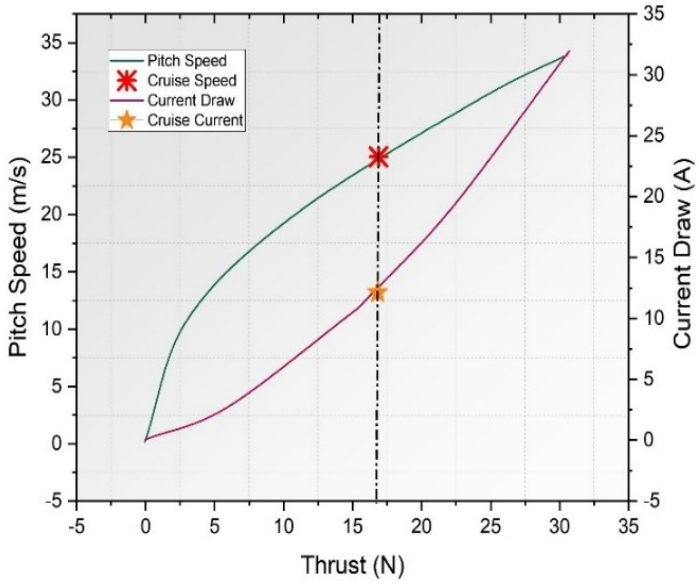

Figure 2. optimal thrust curve.

Table 2. Front motor selection.

Parameter	Values
Type	BLDC (Brushless DC Motor)
Max Thrust	2950 g
Voltage	22.2 V
Propeller Compatibility	24 cm × 15.24 cm
KV Rating	420 RPM/V
Weight	143 g
Maximum Power	680 W

Battery: Despite having a slightly lower energy density than Lithium-Ion batteries, Lithium Iron Phosphate (LiFePO4) batteries are preferred for their improved safety, longer cycle life, and predictable performance qualities. These batteries are appropriate for situations where safety is of the utmost importance since they offer both chemical and thermal stability, which lowers the possibility of thermal runaway. All flying segments had their current draw analyzed and LiFePO4 batteries were found to be adequate for the operational demands of the UAV. The

theoretical flight range and cruise endurance have been recalculated, displaying an endurance of 65 min at cruising and a potential flying range of 110 km. The weight of the battery pack is slightly higher, but this is a trade-off for enhanced safety and lifespan. Selecting the battery parameters is provided in **Table 3**.

$$\eta_{total} = \eta_{propeller}\eta_{motor}\eta_{battery} \tag{41}$$

$$F_{cruise} = \frac{D_{cell}m_{parallel}}{J_{cruise}m_{motors}}\eta_{total} \tag{42}$$

$$Q_{sg} = \upsilon_{cruise}F_{cruise} \tag{43}$$

Table 3. Battery selection.

Parameter	Values
Form Factor	18650 (standard cylindrical size)
Cell Capacity	1500 mAh
Cell Voltage (Nominal)	3.2 V
Cell Discharge (Peak)	3C (4.5 A)
Weight (cell)	45 g
Cell Discharge	1C (1.5 A)

Rear Motor: The Cobra C-5030/16 rear motor is designed to maximize efficiency during hover segments by drawing the least current. Its design ensures the propeller disk diameter doesn't meet the fuselage at an intersection and keeps thrust values near theoretical expectations by maintaining enough disk loading. The motor's KV ranges from 330 to 390 KV, which is perfectly suited for the Cobra C-5030/16, which has a KV rating of 320 RPM/V. The motor was purchased from nearby markets and $eCalc$ was used to confirm the collective propulsion findings, confirming that the practical results align with the developed theoretical formulae. Selecting the Rear Motorparameters is provided in **Table 4**.

Table 4. Rear motor selection.

Parameter	Values
Type	BLDC (Brushless DC Motor)
Propeller Compatibility	50 cm × 15 cm
Maximum Power	1100 W
Max Thrust	5600 g
Weight	198 g

A flying system's tilt technique has to be reliable and rotate 95 degrees when in cruise and 5 odd degrees when in tri-copter mode's vectored yaw. Due to its great rotational efficiency, a gearing approach was used. Spur gear pressure angles were set based on their strength, load-bearing capability, and contact lengths. To eliminate interference, the gear ratio was set at 1:1 and the minimum number of teeth was 19.

$$Y_{min} = \frac{2}{sin^2\phi} \tag{44}$$

3.5. Material selection and preparation

Lightweight materials like XPS and Gff were chosen for their positive features in UAV production. The primary structural elements were built using vacuum-assisted wet layup techniques, ensuring structural integrity and performance. These materials enhance the lightweight aircraft's stability and efficiency.

Extruded polystyrene foam (XPS): Lightweight: Drones need XPS because its lightweight nature implies increased flying duration and effectiveness, Structural Strength: The drone's frame and other parts are supported by the good strength in structure that XPS delivers despite its lightweight construction, Insulation: XPS is an excellent insulator, helping to shield electrical components from changes in temperatures while in flight, Shaping Ease: XPS is readily molded and sculpted, maintaining the structural integrity of the drone's body design while enabling customization.

Glass fiber fabric (Gff): High Strength-to-Weight Ratio: Gff is well-known for having an excellent strength-to-weight ratio, which makes it perfect for contributing little weight while strengthening the drone's construction, Persistence: Gff is extremely robust and can endure external pressures and disturbances encountered during flight, extending the drone's life, Freedom: Because Gff is adaptable and can be shaped into a variety of forms, it allows for greater design freedom when developing aerodynamic structures, Corrosion Resistance: Gff has a high corrosion resistance, which is crucial for drones that could be subjected to a variety of environmental factors.

The UAV is designed for efficient data flow among subsystems, with the Matek Systems F765-WING serving as the autopilot. The u-blox NEO-M8N GPS manages positioning, while the SiK Telemetry Radio facilitates communication between ground control systems and the UAV. External sensors include Voltage Regulators for better power management and Differential Pressure Sensors for airspeed measurements. The Sony RX0 II camera handles visual reconnaissance, while the DJI Ronin-SC gimbal stabilizes images during flight. The Raspberry Pi 4 Model B manages computational tasks, particularly image recognition, while Ubiquiti Bullet M2 Wi-Fi modules ensure robust data transmission across the ad-hoc mesh network. **Figure 3** depicts the architecture of the system. The system is designed for custom operations and offers advanced mission programming and stability controls.

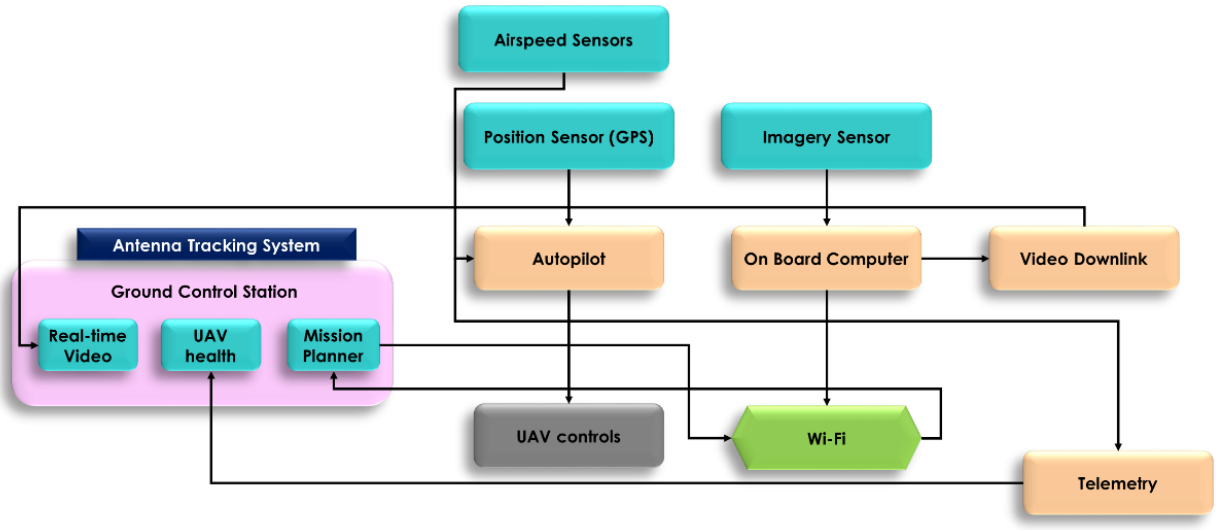

Figure 3. Architecture of the system.

3.6. Open-source software

There are advantages and disadvantages to open-source software. When designing, one must take into account that there are no conventional systems of coordinates or unit systems and there is a lack of universal conceptual comprehension throughout the software. The collaborative nature of open-source software, despite core team oversight, requires significant effort to become familiar with all tools and produce meaningful results. Understanding and changing models/configurations involve user effort, especially when there is a lack of communities, code contributors, and records. To address this challenge, multiple professionals can collaborate to avoid acquiring norms and underlying theories for different software. The accuracy of the outcomes was confirmed through reading relevant literature, running studies concurrently using commercial programs, and computing mistakes.

3.7. Multi-objective Co-evolving Ant Colony Optimization (MC-ACO)

The Multi-Objective Optimization (MC-ACO) framework is intended to manage complicated drone design goals such as weight, durability, cost, and performance indicators such as range and cargo capacity. Its evolutionary technique, which leverages input from many solutions to repeatedly enhance the population of options, is effective in drone design. MC-ACO improves Ant Colony Optimization's effectiveness in exploring and exploiting search areas by successfully navigating the design space of drones. It also aids in managing trade-offs between conflicting goals, such as balancing the drone's weight with its range or cargo capacity. This method is very useful in drone design, as the interplay of several design components may be refined to reach the best balance.

A multi-population approach: The ACO method generates new solutions using just one type of ant and the solutions are controlled by the ant colony size, selection parameter, and convergence parameter. Generally speaking, it is challenging to choose the right parameter values to produce an enhanced ACO algorithm that avoids premature convergence and converges quickly. Consequently, the ACO

algorithm is enhanced by employing a multi-population technique. This approach will separate the ants into elite and common ants. Utilizing a probability selection technique in conjunction with a Gaussian kernel function, the elite ants can produce solutions by gathering knowledge from the solution archive. The elite ants vary in that they have their own set of criteria. Essentially, the elite ants are utilized to increase the ACO algorithm's convergence rate. To prevent falling into a local optimum value, the average value of each dimension and a single Gaussian function are employed by common ants to develop new solutions at a slower pace. Here is a description of the normal ant's Gaussian function.

$$e_M^j(w) = \frac{1}{\sigma_{j,M}\sqrt{2\pi}} e^{-\frac{\left(w-\mu_{j,M}\right)^2}{2\sigma_{j,M}^2}} \tag{44}$$

$$\mu_{j,M} = \sum_{l=1}^{L} T_{j,l} \tag{45}$$

$$\sigma_{j,M} = \xi M \sum_{f=1}^{L} \frac{\left|T_{j,f} - \overline{T}_j\right|}{L-1} \tag{46}$$

In this equation, $e_M^j$is the Gaussian function for regular ants in the j^{th}dimension, $\mu_{j,M}$ is the observed value, and $\sigma_{j,M}$ is the computed average variance. The usual ant rate of convergence is controlled by a constant called ξM, where T_j represents the average value of solutions in the j^{th} region. Regular ants can broaden their search area and improve global search capabilities.

Algorithm 1 MC-ACO

1: **Step 1: Initialize Populations:** Begin with separate populations of elite and common ants, each with distinct roles and parameters.

2: **Step 2: Solution Generation:** Use elite ants to generate new solutions by utilizing a probability selection technique combined with a Gaussian kernel function, leveraging knowledge from the solution archive.

3: **Step 3: Solution Update by Common Ants:** Common ants create new solutions using the Gaussian function, focusing on exploring the search space to avoid local optima.

4: **Step 4: Update Parameters:** For each dimension$j$, calculate the mean $\mu_{j,}$ M, and variance $\sigma_{j,M}$ based on current solutions.

5: **Step 5: Convergence Adjustment:** Control the rate of convergence for common ants using the constantξM, allowing them to effectively expand their search area.

6: **Step 6: Co-evolutionary Interaction:** Enable interactions between sub-populations (elite and common ants) to co-evolve and enhance overall solution quality through collaborative and competitive relationships.

7: **Step 7: Iterate:** Repeat the process, continuously improving the population of solutions until convergence criteria are met or a predetermined number of iterations is reached.

The mechanism of co-evolution: In recent years, a novel evolutionary process has emerged based on co-evolution theory. The process of evolution acknowledges biological variety and highlights specific relationships of dependency between organisms and their surroundings. The notion of co-evolution is utilized to establish

a competitive or cooperative relationship between two or more populations, to enhance optimal performance through collaborative efforts. It highlights how several subpopulations at the moment interact, influence one another, and co-evolve alongside one another. The ACO algorithm incorporates the co-evolution mechanism to facilitate information exchange among sub-populations.

Algorithm 1 presented in the section on Multi-objective Co-evolving Ant Colony Optimization (MC-ACO) may be summarized in a step-by-step fashion to clarify the process.

4. Result and analysis

Python was used to optimize the cost function using an MC-ACO technique with appropriately adjusted weights. The design's libraries and software provide a robust API for creating bespoke loops and performing rapid numerical calculations across multiple processes. The lightweight aircraft geometry and configuration settings are defined using a combination of Python scripts and the initial design inputs, with aerodynamic analysis conducted through JSBSim using a method analogous to the Vortex Lattice Method (VLM). **Figure 4** illustrates the revised process loop for this approach.

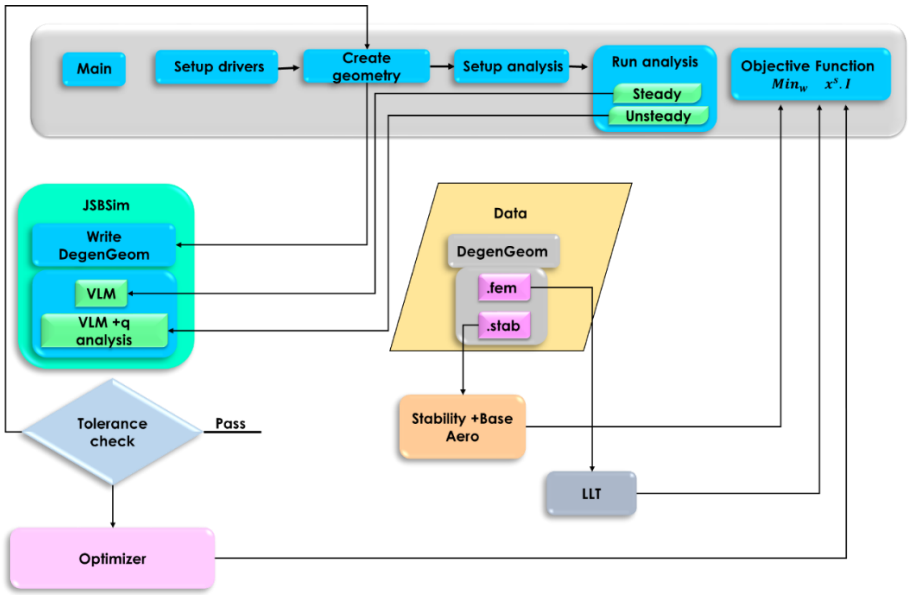

Figure 4. Architectural optimization.

Flight testing

The Matek Systems F765-WING autopilot was tested to improve its flight dynamics and fine-tune the system. The UAV was adjusted to perform optimally in hover and cruise modes using advanced firmware from ArduPlane and QGroundControl for mission planning. Key flight parameters were calibrated, including lowering to stabilize pitch, increasing to enhance yaw control during transitions, and reducing overall vibrations. However, further tests exposed complex behaviors in the VTOL system dynamics, particularly under vectored yaw motions. The UAV's financial limits hampered the performance of the 3D-printed

components utilized in the tilt system, contributing to mechanical vulnerabilities. Additionally, electronic components frequently overheated or experienced interference, exacerbated by the high current demands of the motors.

Subsequent debugging efforts were extensive, sourced from the Arduplane community forums, to overcome technical challenges. However, the escalating costs associated with repairs and replacement parts ultimately curtailed comprehensive range testing. The revised system architecture includes upgraded components like the u-blox NEO-M8N GPS for precise localization, SiK Telemetry Radio for improved communication, and a Sony RX0 II camera paired with a DJI Ronin-SC gimbal for superior aerial imaging and stabilization. The Raspberry Pi 4 Model B efficiently handles onboard computing tasks, while the Ubiquiti Bullet M2 Wi-Fi modules ensure reliable data communication across the UAV's ad-hoc mesh network.

The MC-ACO is a design optimization method used for optimizing lightweight aircraft structures and aeroelasticity. It has been run for 80 generations, with design solutions increasing and reaching a plateau in **Figure 5**. The algorithm does not address structures and aeroelasticity, so a feasible design is chosen based on experienced engineering judgment. **Table 5** provides specific geometry for the chosen design and to guarantee dependability, a safety factor is added when estimating weight. The vortex lattice method, implemented within JSBSim, is effective for lift analysis but does not accurately determine overall drag. The geometry optimization using MC-ACO primarily focuses on the cruise phase of flight, which is critical for overall performance. Human oversight is essential to guide the process and eliminate suboptimal or non-convex geometries.

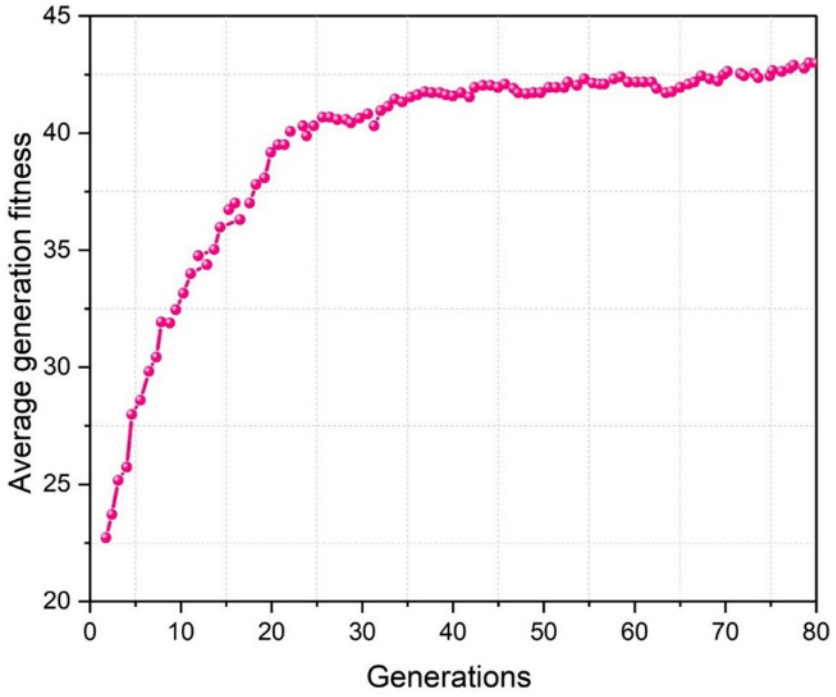

Figure 5. Optimization results.

Table 5. Lightweight aircraft parameters.

Parameter	Values
Leading edge sweep	30°
Relative twist	−1°
Wing incidence	4°
Taper ratio	0.675
Aspect ratio	8.0
Wing area	0.450 m^2
Power loading	3.0 kg/kW
Wing loading	150 N/m^2

Figure 6 displays peak D_k/D_c values, stall qualities, and Reynold's number during the initial aircraft performance estimate using XFOIL. This data aids in obtaining static stability parameters for aircraft design, enabling informed decisions about aerodynamic performance, particularly lift and drag characteristics. The data aids in selecting a reflexed airfoil and guides optimization to achieve desired performance goals. A graph or curve showing the drag fluctuation at various angles of attack or airspeeds, highlighting stalling, is shown in **Figure 6A**, which also shows the peak drag coefficient ratio (D_k/D_c) under various flight situations. Stall characteristics show the crucial velocities or angles at which drag rises and lift decreases. Plots showing Reynolds number changes throughout flying situations and lightweight aircraft configurations are shown in **Figure 6B**. These plots may be used to forecast flow patterns in fluid mechanics and to influence aerodynamic performance in aircraft design.

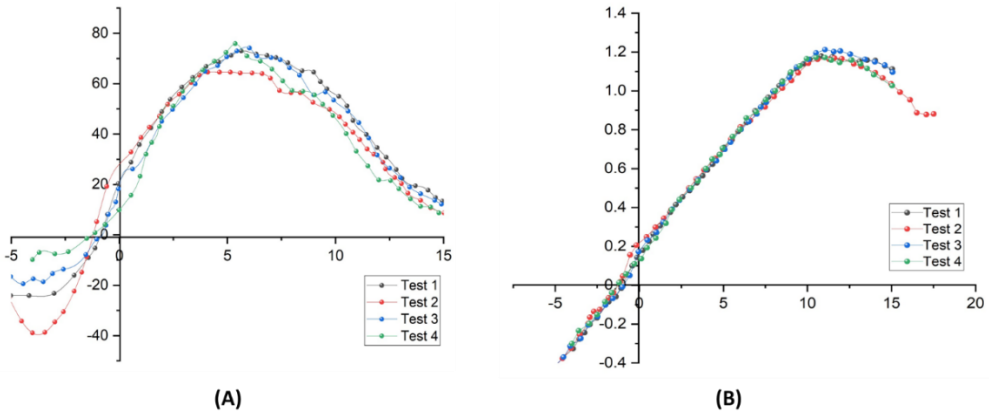

Figure 6. (A) highlighting stall qualities; **(B)** Reynolds number varies under flight conditions.

5. Conclusion

This research did the task successfully and has an innovative drone design model that utilizes multi-objective optimization together with lightweight materiality specifically for VTOL and FW configurations. MC-ACO alongside materials such as XPS and Gff has proven to be a viable option for addressing this issue. Utilized entirely open-source software for both design and assessment, facilitating the technology's swift adoption and expansion without incurring the exorbitant expenses

associated with proprietary instruments. Therefore, the study has demonstrated a possibly practical solution for solving the trade-offs among drone parameters, including range, payload, and operation in swarms. The application of low-fidelity prototypes, being enabled by open-source software, was found to be valuable for speedy prototyping when time was a constraint and, in this way, a cost-effective approach to drone design was revealed. The results show that low-fidelity architecture is an excellent place to start when prototyping in a constrained amount of time. The technical limitations of using free software are covered in the paper's conclusion, along with some useful considerations for flying test drones with hybrid configurations. Biomechanics into the design system could improve the operational performance of drones. Nevertheless, the study also points out drawbacks related to the technical restrictions associated with the free software as well as the practical difficulties involved during the flight tests of drones with hybrid constructions. Such information arises as a roadmap for the more refined stage of the design process and calls for further research and development to improve the utility and applicability of the drone, especially in sectors where this kind of technology is adopted.

Limitation and future scope

The main challenges are the technical constraints of free software used, points of inaccuracies involved in low-fidelity prototypes, and difficulties in testing and validation of hybrid drone configurations under various task situations. We will put much effort into developing high-fidelity prototypes, improving the algorithm accuracy, enhancing software functions, and conducting extensive field tests to make sure the drone performance will work under any environmental condition.

Author contributions: writing—original draft preparation, WJ; writing—review and editing, PR; visualization, PR; supervision, PR. All authors have read and agreed to the published version of the manuscript.

Ethical approval: Not applicable.

Conflict of interest: The authors declare no conflict of interest.

References

1. Hildmann H, Kovacs E. Review: Using Unmanned Aerial Vehicles (UAVs) as Mobile Sensing Platforms (MSPs) for Disaster Response, Civil Security and Public Safety. Drones. 2019; 3(3): 59. doi: 10.3390/drones3030059
2. Emimi M, Khaleel M, Alkrash A. The Current Opportunities and Challenges in Drone Technology. Int. J. Electr. Eng. And Sustain. 2023; 1(3): 74-89.
3. Dams B, Sareh S, Zhang K, et al. Remote three-dimensional printing of polymer structures using drones. Proceedings of the Institution of Civil Engineers - Construction Materials. 2017; 1-31. doi: 10.1680/jcoma.17.00013
4. Rajak D, Pagar D, Menezes P, et al. Fiber-Reinforced Polymer Composites: Manufacturing, Properties, and Applications. Polymers. 2019; 11(10): 1667. doi: 10.3390/polym11101667
5. Sun J, Cai F, Tao D, et al. Enhanced Thermal Insulation of the Hollow Glass Microsphere/Glass Fiber Fabric Textile Composite Material. Polymers. 2021; 13(4): 505. doi: 10.3390/polym13040505
6. Zhu H, Nie H, Zhang L, et al. Design and assessment of octocopter drones with improved aerodynamic efficiency and performance. Aerospace Science and Technology. 2020; 106: 106206. doi: 10.1016/j.ast.2020.106206
7. Chen Z, Zhang Z, Xie J, et al. Metaheuristic optimization method for compact reactor radiation shielding design based on genetic algorithm. Annals of Nuclear Energy. 2019; 134: 318-329. doi: 10.1016/j.anucene.2019.06.031

8. Osaba E, Villar-Rodriguez E, Del Ser J, et al. A Tutorial On the design, experimentation and application of metaheuristic algorithms to real-World optimization problems. Swarm and Evolutionary Computation. 2021; 64: 100888. doi: 10.1016/j.swevo.2021.100888
9. Badini S, Regondi S, Pugliese R. Unleashing the Power of Artificial Intelligence in Materials Design. Materials. 2023; 16(17): 5927. doi: 10.3390/ma16175927
10. Cañas JM, Martín-Martín D, Arias P, et al. Open-Source Drone Programming Course for Distance Engineering Education. Electronics. 2020; 9(12): 2163. doi: 10.3390/electronics9122163
11. Kopar M, Yıldız AR, Yıldız BS. Optimum design of a composite drone component using slime mold algorithm. Materials Testing. 2023; 65(12): 1857-1864. doi: 10.1515/mt-2023-0245
12. Skarka W, Jałowiecki A. Automation of a Thin-Layer Load-Bearing Structure Design on the Example of High Altitude Long Endurance Unmanned Aerial Vehicle (HALE UAV). Applied Sciences. 2021; 11(6): 2645. doi: 10.3390/app11062645
13. Pecho P, Ažaltovič V, Kandera B, et al. Introduction study of design and layout of UAVs 3D printed wings in relation to optimal lightweight and load distribution. Transportation Research Procedia. 2019; 40: 861-868. doi: 10.1016/j.trpro.2019.07.121
14. Yilmaz F, Şahin M, Gürses E. Weight reduction of an unmanned aerial vehicle pylon fitting by topology optimization and additive manufacturing with electron beam melting. Journal of Additive Manufacturing Technologies. 2021; 1(2). doi: 10.18416/JAMTECH.2111553
15. Yap YL, Toh W, Giam A, et al. Topology optimization and 3D printing of micro-drone: Numerical design with experimental testing. International Journal of Mechanical Sciences. 2023; 237: 107771. doi: 10.1016/j.ijmecsci.2022.107771
16. Balayan A, Mallick R, Dwivedi S, et al. Optimal Design of Quadcopter Chassis Using Generative Design and Lightweight Materials to Advance Precision Agriculture. Machines. 2024; 12(3): 187. doi: 10.3390/machines12030187
17. Maricic S, Haber IM, Veljovic I, et al. Implementation of optimum additive technologies design for unmanned aerial vehicle take-off weight increase. Eureka: Physics and Engineering. 2020; (6): 50-60. doi: 10.21303/2461-4262.2020.001514
18. García-Gascón C, Castelló-Pedrero P, García-Manrique JA. Minimal Surfaces as an Innovative Solution for the Design of an Additive Manufactured Solar-Powered Unmanned Aerial Vehicle (UAV). Drones. 2022; 6(10): 285. doi: 10.3390/drones6100285
19. Maity R, Mishra R, Kumar Pattnaik P, et al. Selection of sustainable material for the construction of UAV aerodynamic wing using MCDM technique. Materials Today: Proceedings. doi: 10.1016/j.matpr.2023.12.025
20. Dinovitzer M, Miller C, Hacker A, et al. Structural Development and Multiscale Design Optimization of Additively Manufactured UAV with Blended Wing Body Configuration Employing Lattice Materials. AIAA Scitech 2019 Forum. doi: 10.2514/6.2019-2048
21. Xiao R, Li X, Jia H, et al. 3D printing of dual phase-strengthened microlattices for lightweight micro aerial vehicles. Materials & Design. 2021; 206: 109767. doi: 10.1016/j.matdes.2021.109767
22. Elelwi M, Pinto FS, Botez RM, et al. Multidisciplinary Optimization for Weight Saving in a Variable Tapered Span-Morphing Wing Using Composite Materials—Application to the UAS-S4. Actuators. 2022; 11(5): 121. doi: 10.3390/act11050121
23. Jayakumar SS, Subramaniam IP, Stanislaus Arputharaj B, et al. Design, control, aerodynamic performances, and structural integrity investigations of compact ducted drone with co-axial propeller for high altitude surveillance. Scientific Reports. 2024; 14(1). doi: 10.1038/s41598-024-54174-x
24. Raja V, AL-bonsrulah HAZ, Gnanasekaran RK, et al. Design and advanced computational approaches based comprehensive structural parametric investigations of rotary-wing UAV imposed with conventional and hybrid computational composite materials: A validated investigation. Frontiers in Materials. 2023; 10. doi: 10.3389/fmats.2023.1096839
25. Nvss S, Esakki B, Yang LJ, et al. Design and Development of Unibody Quadcopter Structure Using Optimization and Additive Manufacturing Techniques. Designs. 2022; 6(1): 8. doi: 10.3390/designs6010008